ISSN 2348-1196 (print)
International Journal of Computer Science and Information Technology Research ISSN 2348-120X (online)
Vol. 2, Issue 3, pp: (328-338), Month: July - September 2014, Available at: www.researchpublish.com

FACIAL IDENTIFICATION FROM SCIENTIFIC VISUALIZATION OF MAGNETIC RESONANCE IMAGING DATA

[1]Ms. A. Sivasankari, [2] Mrs. G. Sangeethalakshmi, [3]Mrs. K. Elakkya

1,2,3Department of Computer Science, D.K.M College for Women, Vellore, Tamil Nadu, India

Abstract: **The technique of functional magnetic resonance imaging is rapidly moving from one of technical interest to wide clinical application. However, there are a number of questions regarding the method that need resolution. Some of these are investigated in this thesis. High resolution FMRI is demonstrated at 3.0 T, using an interleaved echo planar imaging technique to keep image distortion low. The optimum echo time to use in FMRI experiments is investigated using a multiple gradient echo sequence to obtain six images, each with a different echo time, from single free induction decay. Magnetic resonance imaging (MRI) is a technique which finds use in the neurosciences both as an anatomical and functional localization tool. The traditional uses of MRI for structural analysis, such as are commonly found in medicine, can be adapted to serve in place of histological studies for identifying areas of interest in the cortex. Functional MRI (FMRI) is a rapidly developing tangent of MRI which can be used alone or in tandem with classical electrophysiological experiments to investigate neural activity. Although developed intensely for clinical and scientific studies in human subjects, MRI and FMRI have been used increasingly in the non-human primate. This document contains work exemplifying the use of FMRI in both species and methods for pre- and post-surgical anatomical MRI in the non-human primate. The chance probability that an observer could match a photograph with its 3-D MR image was 1 in 40 (0.025), and we considered 4 successes out of 40 (4/40, 0.1) to indicate that a subject could iden- tify persons' faces from their 3-D MR images**

Keywords: **Biomedical imaging, face recognition, magnetic resonance imaging, privacy. MRI, FMRI. 3-D Images.**

I. INTRODUCTION

Volumetric reconstructions of computed tomography (CT) and MRI data have become commonplace in both research and clinical radiology. Multicenter clinical trials require widespread information and image sharing. The Health Insurance Portability and Accountability Act of 1996 (HIPAA) Privacy Rule requires that in most instances, individually iden- tifiable health information may not be disclosed or used for

research unless that information is properly de-identified. De-identification requires the removal of 18 specified categories of identifiers that may be associated with an individual's protected health information (PHI). When dealing with volumetric medical imaging data, however, there is at present a certain level of ambiguity in interpretation of the HIPAA privacy statutes.

The Privacy Rule states: if an image could be used "alone or in combination with other information to identify an individual who is a subject of the information," it should be considered an identifier. The phrase "Full face photographic images and any comparable images" is consistently used throughout the text of 45 CFR Part 164. Unfortunately, the legislation is unclear: Is a three-dimensional (3-D) facial reconstruction from CT or MRI data

At present, little scientific data are available to prove that facial images reconstructed from volumetric magnetic resonance (MR) studies are identifiable in the sense implied by the HIPAA Privacy Rule. Chen et al. explored this question using 3-D reconstructions from CT data. Although they observe that "image reviewers were surprisingly poor at being able to match a 3D surface reconstructed image with candidate patient photographs," their preliminary data from a relatively small pilot study shows that, in fact, 57% of the time an observer can correctly match a photograph and a facial

reconstruction from CT. The real question is whether a human observer can consistently identify from a standard clinical or research facial reconstruction the human being who was the subject of the CT or MRI.

A. Background of the Research

Person authentication using fingerprint or voice biometric traits has increasingly being deployed for day to day security and surveillance applications. However, one of most acceptable non-intrusive physiological attribute to authenticate is "face".

The Privacy Rule states: if an image could be used "alone or in combination with other information to identify an individual who is a subject of the information," it should be considered an identifier. The phrase "Full face photographic images and any comparable images" is consistently used throughout the text of 45 CFR Part 164. Unfortunately, the legislation is unclear: Is a three-dimensional (3-D) facial reconstruction from CT or MRI data a "comparable image" for the purposes of Identification. This ambiguity has been interpreted by some researchers and covered entities to imply that volumetric CT and MRI data sets must be modified or "de-faced" to eliminate the possibility of rendering the face of the human subject. A brief Internet and telephone survey of ten medical imaging research institutions determined that three had an official policy that 3-D image reconstructions are equivalent to photographs, and therefore, must be modified prior to release, four institutions had an official policy that such modification of medical images is not required, and three institutions had no official policy on the matter.

B. Facial Recognition System

A facial recognition system is a computer application for automatically identifying or verifying a person from a digital image or a video frame from a video source. One of the ways to do this is by comparing selected facial features from the image and a facial database. It is typically used in security systems and can be compared to other biometrics such as fingerprint or eye iris recognition systems. (CIA). Since confidentiality, integrity and authenticity, beside Denial of Service (DoS) attack, are major aspects of security, there is a need to understand how they are addressed in a converged IEEE 802.x wireless network.

II. THIRD GENERATION TECHNIQUES

A. Traditional

Some facial recognition algorithm identifies facial features by extracting landmarks, or features, from an image of the subject's face. For example, an algorithm may analyze the relative position, size, and/or shape of the eyes, nose, cheekbones, and jaw. These features are then used to search for other images with matching features. Other algorithms normalize a gallery of face images and then compress the face data, only saving the data in the image that is useful for face recognition. A probe image is then compared with the face data. One of the earliest successful systems is based on template matching techniques applied to a set of salient facial features, providing a sort of compressed face representation. Popular recognition algorithms include Principal Component Analysis using eigenfaces, Linear Discriminate Analysis, Elastic Bunch Graph Matching using the Fisher face algorithm, the Hidden Markov model, the Multiline Subspace Learning using tensor representation, and the neuronal motivated dynamic link matching.

B. 3-Dimensional Recognition

A newly emerging trend, claimed to achieve improved accuracies, is three-dimensional face recognition. This technique uses 3D sensors to capture information about the shape of a face. This information is then used to identify distinctive features on the surface of a face, such as the contour of the eye sockets, nose, and chin.

One advantage of 3D facial recognition is that it is not affected by changes in lighting like other techniques. It can also identify a face from a range of viewing angles, including a profile view. Three-dimensional data points from a face vastly improve the precision of facial recognition. 3D research is enhanced by the development of sophisticated sensors that do a better job of capturing 3D face imagery. The sensors work by projecting structured light onto the face. Up to a dozen or more of these image sensors can be placed on the same CMOS chip—each sensor captures a different part of the spectrum.

C. Skin Texture Analysis

Another emerging trend uses the visual details of the skin, as captured in standard digital or scanned images. This technique, called skin texture analysis, turns the unique lines, patterns, and spots apparent in a person's skin into a mathematical space. Tests have shown that with the addition of skin texture analysis, performance in recognizing faces can increase 20 to 25 percent. Also viscosity of a sample plays a role on the quality of the results. In this experiment you are going to perceive an Earth Field Nuclear Magnetic Resonance (EFNMR), which is the same thing as an MRI with only one difference, and that being that EFNMR uses the earth magnetic field whereas MRI has a huge magnet 10,000 times stronger than the earth's magnetic field.

D. Efnmr

The nuclei of atoms are aligned with the Earth's Magnetic Field because that is the only magnet we have by using this apparatus. Each time we send a pulse to the spectrometer, we are sending electricity to the probe. This causes the nuclei to position themselves perpendicular to the original status they had which was alignment with the magnetic field. So the nuclei originally are aligned parallel to the magnetic field and after a pulse they are positioned perpendicular to the earth's magnetic field.

Fig. 1 EFNMR components Tools

We will concentrate only on the second image to the right, the Magnitude spectrum. Notice there is now an upside down peak located somewhat in the center of the spectrum. To properly adjust the capacitance, we must increase or decrease the capacitance to ensure the upside down peak is in the center of the spectrum. Increasing the capacitance moves the upside down peak to the right, and decreasing the capacitance moves the upside down peak to the left. Therefore, we must

ISSN 2348-1196 (print)
International Journal of Computer Science and Information Technology Research ISSN 2348-120X (online)
Vol. 2, Issue 3, pp: (328-338), Month: July - September 2014, Available at: www.researchpublish.com

increase the capacitance to center the upside down peak in our example. Thus, I will change the capacitance from 17.09 to the max at 17.15. The following image shows the results.The research thesis investigated the security issues on a converged IEEE 802.x wireless network. The investigation emanated from the problem statement above and included an analysis of the inherent security protocols and mechanisms thereby making some recommendation to implement a secure and robust security framework.

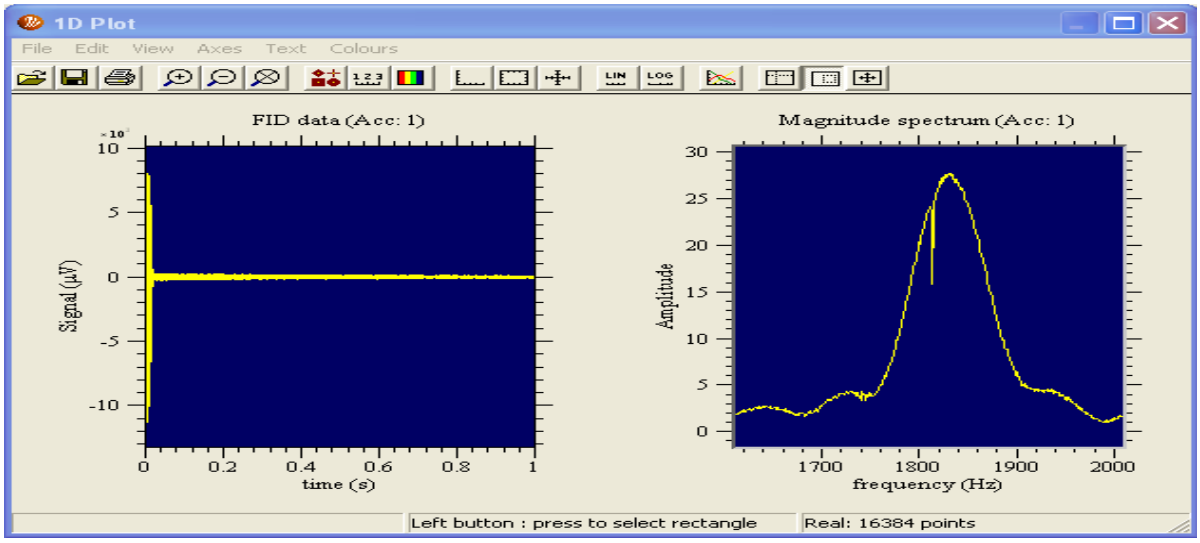

Fig 2 Rating of MRI

III. 3D RECONSTRUCTION OF IMAGES

A. MRI

MRI has a wide range of applications in medical diagnosis and there are estimated to be over 25,000 scanners in use worldwide. MRI has an impact on diagnosis and treatment in many specialties although the effect on improved health outcomes is uncertain. Since MRI does not use any ionizing radiation its use is recommended in preference to CT when either modality could yield the same information. MRI is in general a safe technique but the numbers of incidents causing patient harm have risen. Contraindications to MRI include most cochlear implants and cardiac pacemakers, shrapnel and metallic foreign bodies in the orbits, and some ferromagnetic surgical implants. The safety of MRI during the first trimester of pregnancy is uncertain, but it may be preferable to alternative options. The sustained increase in demand for MRI within the healthcare industry has led to concerns about cost effectiveness and over diagnosis.

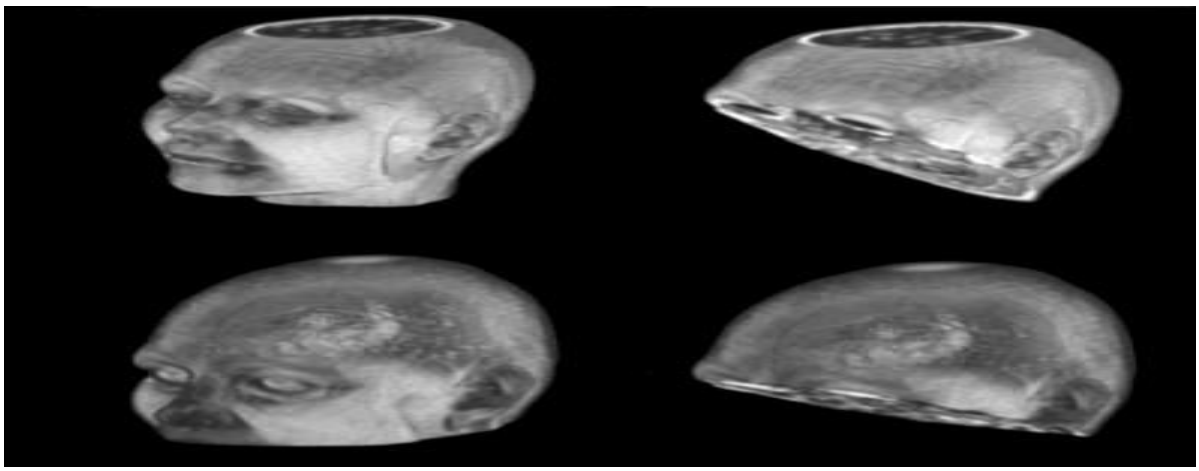

Fig. 3 3D Reconstruction of a Images

1. They do not involve exposure to radiation, so they can be safely used in people who may be vulnerable to the effects of radiation, such as pregnant women and babies.

2. They are particularly useful for showing soft tissue structures, such as ligaments and cartilage, and organs such as the brain, heart and eyes.
3. They can provide information about how the blood moves through certain organs and blood vessels, allowing problems with blood circulation, such as blockages, to be identified.

B. CT Scan

Computed Tomography(CT) of the head or Computed Axial Tomography (CAT) scanning uses a series of x-rays of the head taken from many different directions.[1] Typically used for quickly viewing brain injuries, CT scanning uses a computer program that performs a numerical integral calculation (the inverse Radon transform) on the measured x-ray series to estimate how much of an x-ray beam is absorbed in a small volume of the brain. Typically the information is presented as a series of cross sections of the brain.

Computed tomography (CT) has become the diagnostic modality of choice for head trauma due to its accuracy, reliability, safety, and wide availability. The changes in microcirculation, impaired auto-regulation, cerebral edema, and axonal injury start as soon as head injury occurs and manifest as clinical, biochemical, and radiological changes. Proper therapeutic management of brain injury is based on correct diagnosis and appreciation of the temporal course of the disease process. CT scan detects and precisely localizes the intracranial hematomas, brain contusions, edema and foreign bodies. Because of the widespread availability of CT, there is reduction in arteriography, surgical intervention and skull radiography. MR temperature mapping are reviewed. Special attention was paid to sensitivity, linearity of the effects with temperature, their dependence on coagulation or field strength, and the question of whether absolute or relative temperature is measured.

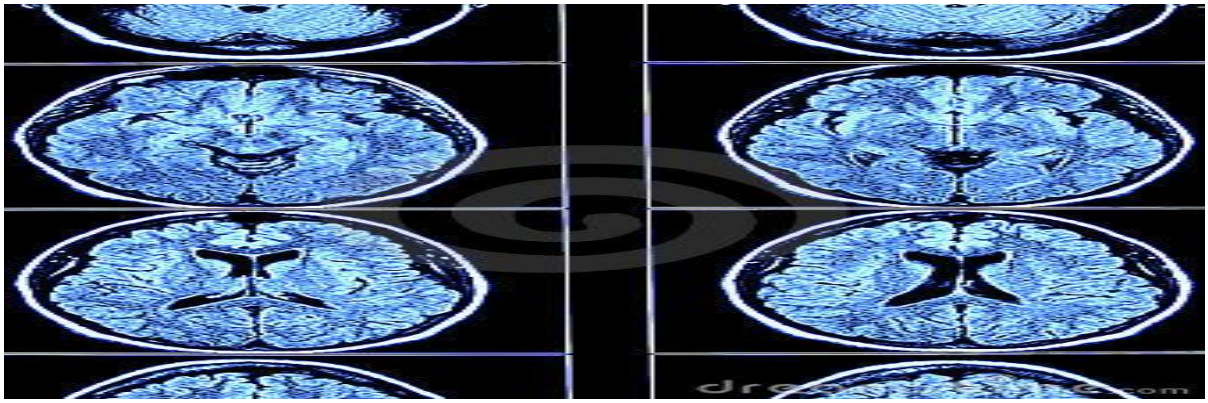

Fig. 4 CT Scan Report

C. Performance

Performance data are summarized in Additional file 1. Behavioral measures of accuracy (retrieval task) and reaction time (encoding and retrieval tasks) were acquired for all subjects. In encoding task, there were no differences in reaction time between PTSD patients and comparison subjects ($Z = 0.52$, $p > 0.05$) (see Additional file 1). In the retrieval task, patients tend to have lower accuracy in recognizing targets and longer response time. For instance, there were significant differences in reaction time ($Z = 4.21$, $P < 0.001$) and in response bias ($X = 16.98$, $P < 0.001$). Here is no difference in performance based on whether the facial expression for the probe image acquisition is matched to the facial expression for the gallery image acquisition.

IV. SYSTEM ANALYSIS

The 11 infants who had a conventional brain MRI with an obvious or possible infarction were included in this study. DWI and MRS detected additional areas in one infant and more prominent regions of abnormality than initially seen on MRI were found with DWI in two. The clinical information is summarized in Table 1, initial MR data in Table 2, and follow-up MR data in. The magnetic resonance (MR) examination included conventional T1- and T2-weighted MRI, DWI, MRA, and MRS. The DWI used an echo planar pulse sequence with an echo time (TE)=96 ms, 3 mm slice thickness, and a diffusion factor b=1,000 seconds/mm2. Single-voxel MR spectra were recorded with a double-spin-echo sequence, TE=144 milliseconds and repetition time of 1600 milliseconds. Some spectra also were recorded with TE=288

ISSN 2348-1196 (print)
International Journal of Computer Science and Information Technology Research ISSN 2348-120X (online)
Vol. 2, Issue 3, pp: (328-338), Month: July - September 2014, Available at: www.researchpublish.com

milliseconds, or with a stimulated-echo sequence and TE=20 milliseconds. All infants had a brain MRI exam between 2 and 8 days after birth, and eight had a second exam at least 6 weeks later. MR spectra were acquired in 10 of the 19 exams, including spectra of the stroke region in six initial exams and four follow-up exams. Peak areas for NAA (N-acetyl aspartame), creative, chorine, and lactate were measured. A spectrum from normal-appearing brain contra lateral to the infarct often was obtained as a control to the stroke region.

Typical transfer rates for user data are 5 Mbit/s. For difficult propagation conditions (i.e. larger range, interference,), the system uses link adaptation to lower transfer rates. The next table gives an overview about the different data rates on the physical layer of 802.11b systems and the corresponding maximum range for open environments (i.e., outdoor or large halls) and for ―closed‖ environments (i.e. indoor) Infants 2 and 3 had clinical evidence of prenatal difficulties and both had MRI evidence of bilateral border zone infarction suggesting a global ischemia. Infant 2 had a probable bilateral ACA-MCA and MCA-PCA infarct on MRI, and the DWI showed obvious abnormalities in this region. MRS revealed a near absence of metabolites in the infarct and reduced NAA in the right basal ganglia. This baby had Apgar scores of 0 and 1 and a perinatal seizure. The parents did not agree to follow-up imaging and the patient developed microcephaly. These findings are consistent with hypoxia or a global perfusion deficit, or possibly both. Infant 3 had decreased fetal movement 2 days before birth, Apgar scores of 3, 5, and 7, and a possible seizure on day 1 after birth. Some of the MRI, DWI, and MRS data from this infant were published as part of a study of neonatal hypoxia/ischemia.18 DWI revealed a large bilateral parieto-occipital ischemic area, and MRS of this region revealed a large lactate signal. A large lactate signal also was found in the right basal ganglia, as commonly seen with perinatal hypoxia/ischemia.18 The borderzone location of the infarct and the basal ganglia lactate signal are consistent with global ischemia.

Infant 4 had probable bilateral PCA infarcts on MRI and a possible small right basal ganglia abnormality. DWI showed only bilateral PCA abnormalities with an elevated lactate on occipital MRS. Basal ganglia MRS revealed an NAA level near the lower limit of normal and no detectable lactate. MRA was interpreted as showing an insufficiency of the vertebrobasilar circulation. This infant had Apgar scores of 7 and 9 and fetal distress resulting in an emergency caesarean section.

Table 1 Numbers Of Subjects And Correct Matches

Number Correct	*Number Subjects*	*Percent*	*Lower CI**	*Upper CI*
0	5	0.06	0.03	0.14
1	14	0.18	0.11	0.28
2	10	0.13	0.07	0.22
3	17	0.22	0.14	0.33
4	13	0.17	0.10	0.27
5	4	0.05	0.02	0.13
6	9	0.12	0.06	0.21
8	2	0.03	0.01	0.09
9	3	0.04	0.01	0.11

*CI = 95% confidence interval.

A. MRI Temperature Methods

Temperature MRI Based on the T1 Relaxation

The variation in T1 with temperature can be described by the following relationship (10,17,25,26):D.

$$T_1 = T_1(\infty)e^{-E_a(T_1)/kT} \qquad (1)$$

where Ea (T1) is the activation energy of the relaxation process, k is the Boltzmann constant, and T is absolute temperature. A description of the molecular processes giving rise to temperature-dependent T1 is beyond the scope of this paper. We mention here only that exchange processes between mobile bulk water and relatively immobilized water at surfaces of proteins and membranes play an important role. Within a small temperature range T1 is linearly dependent on temperature. However, both the T1 and its temperature dependence differ between tissues. Nonlinear effects have been

observed in particular when coagulation occurs (27–29). This is not surprising since exchange processes and effective tumbling rates of water may be influenced drastically. Activation energies have been described between 0.6 and 1.5 eV for the T1 dependency on temperature for different tissue types leading to changes on the order of 1%/°C (30).
For example, the signal intensity in RF-spoiled gradient-echo imaging results from partial recovery of magnetization during the short TR periods and can be used to assess T1 changes (26). Assuming a linear temperature dependence of T1 with temperature T expressed as

$$T_1 = T_{1,\mathrm{ref}} + m(T - T_{\mathrm{ref}}) \qquad (2)$$

where *m* is the tissue-specific temperature dependence of T1, the temperature can be calculated from the dependence of signal intensity *S* as for RF-spoiled gradient- echo sequences:

$$\Delta T = T - T_{\mathrm{ref}}$$

$$= -\frac{S - S_{\mathrm{ref}}}{S_{\mathrm{ref}}} \frac{1}{\dfrac{mT_R(1-\cos\alpha)E}{(1-E)(1-\cos\alpha E)T_{1,\mathrm{ref}}^2} + \dfrac{1}{T_{\mathrm{ref}}}}$$

$$\text{where } E = e^{-T_R/[T_{1,\mathrm{ref}} + m(T - T_{\mathrm{ref}})]}. \qquad (3)$$

The subscript "ref" indicates the value for the reference temperature, and & is the flip angle. Note that the change in signal intensity depends not only on T1, but also on T2 and flip angle. The flip angle should be rather high, close to or even above the Ernst angle, to provide sufficient T1 sensitivity. Absolute temperature measurements are thus not practical with such methods. Alternatively, other methods have been proposed, for example, an inversion of magnetization followed by repeated readouts of the recovery process based on small flip angle excitations (31). The method is very fast but suffers from limited SNR. The inversion can also be followed by a long, single-shot fast spin-echo train (32,33). Only one recovery time is then feasible. The signal intensity dependence for inversion recovery measurements on T1 is given by

$$S(t) \approx 1 - 2e^{-t/T1} + e^{-TR/T1}. \qquad (4)$$

V. EVALUATION RESULT

A. Encoding Task

Additional file 2 presents local maxima for encoding task. As in previous studies [38-40], the comparison subjects had extensive frontal activation, including bilateral Broca's area (Brodmann's area 6), right frontal pole (Brodmann's area 10), left dorsolateral prefrontal cortex (Brodmann's area 46) and bilateral inferior frontal Gyrus (Brodmann's area 47). The comparison subjects also had activation in the right cingulate Gyrus (Brodmann's area 31), bilateral anterior cingulate (Brodmann's area 24, 25), bilateral parahippocampal (Brodmann's area 30), left hippocampus and bilateral insular cortex (Brodmann's area 13). Like the comparison subjects, the patients activated the bilateral Broca's area (Brodmann's area 6), left dorsolateral cortex (Brodmann's area 46), left hippocampus, left insular (Brodmann's area 13) and bilateral parahippocampal (Brodmann's area 34, 35). However, the patients did not activate the right cingulate Gyrus (Brodmann's area 31), bilateral anterior cingulate (Brodmann's area 24, 25), and the right insular cortex (Brodmann's area 13).

B. Retrieval Task

Additional file 3 presents local maxima for retrieval task. The comparison subjects had extensive prefrontal cortex activation, including activation in the right superior pole (Brodmann's area 10), and bilateral Broca's area (Brodmann's area 6, 9). The comparison subjects also showed bilateral activation of cingulate Gyrus (Brodmann's area 24, 31), left activation of parahippocampal Gyrus (Brodmann's area 36), bilateral activation of hippocampus and ICs. Patients with PTSD also had activation in the right superior frontal Gyrus (Brodmann's area 6), bilateral activation of middle frontal Gyrus (Brodmann's area 9, 10), left inferior frontal Gyrus (Brodmann's area 44) and right parahippocampal Gyrus

(Brodmann's area 30). However, in the patients group, there were no significant activations in bilateral cingulate Gyrus, bilateral hippocampus and bilateral ICs.

Fig 5 Retrieval Task

This information is not meant to replace the advice of any physician or qualified health professional. The information provided by Cerebra is for information purposes only and is not a substitute for medical advice or treatment for any medical condition. You should promptly seek professional medical assistance if you have concerns regarding any health issue

VI. RESULT AND DISCUSSION

One hundred and two subjects were registered on the Website. One Asian female recorded her age as 0. Of the remaining 101 subjects, the ages were nonnormally distributed with more young subjects than old subjects (Shapiro–Wilk W test P < 0.01). The youngest subject was 17 and the oldest 62, with a median age of 39 (95% CI = 34 to 46). Forty-one of the 102 subjects (40%) were female and 61 of 102 (60%) were male. Eighty-nine of the 102 subjects (87%) were white, 6 (6%) were Asian, 2 (2%) were African American, and 5 (5%) were others. Only 79 of the 102 (77%) subjects attempted to complete the task—that is, 23 of the 102 subjects (23%) did not per-form a single match. For two of the subjects who did perform matches, there were browser problems and their data were not recorded, and therefore, not available for analysis. For the remaining 77 subjects, the distribution of numbers of photographs that the subjects attempted to match were highly negatively skewed (Shapiro–WilkWtestP <0.01), with 47 of 77 subjects (61%) attempting to match all 40 photographs.

Two subjects attempted to match only one photograph. The median number of attempted matches was 40 (95% CI = 39 to 40). The number of correct matches was positively skewed (Shapiro–Wilk Wtest P <0.01), with a range from 0 to 9, a median value of 3 (95% CI = 3 to 4), and with 31 of 77 (40%) subjects having four or more correct answers (see Table I). The exact Blyth–Still– Casella 95% CI for a success rate of 0.1 (4 of 40 successes) is 0.03–0.23. A success rate of 0.1 is significantly different (P = 0.02) from 0.025 (null hypothesis success rate). Forty percent of the subjects (31 of 77) were able to successfully match photographs with MR images (that is, their success rates were higher than our null hypothesis

ISSN 2348-1196 (print)
International Journal of Computer Science and Information Technology Research ISSN 2348-120X (online)
Vol. 2, Issue 3, pp: (328-338), Month: July - September 2014, Available at: www.researchpublish.com

success rate of 0.025, Table II). The Blyth–Still–Casella 95% CI for the 40% success rate was 29%–52%, and the 40% success rate was significantly higher ($P < 0.001$) than our null hypothesis success rate of 1 in 10 (0.10).

Digital photographs were similarly read into Analyze, resized to a standard presentation, and mapped to the same grayscale as theMRdata. All images were adjusted to the same grayscale because colorization of MR reconstructions is arbitrary. Because existing research image sets were used, approximately half of the subjects were wearing an EEG electrode cap when the MR data were collected. Fig. 1 illustrates the type of data used.

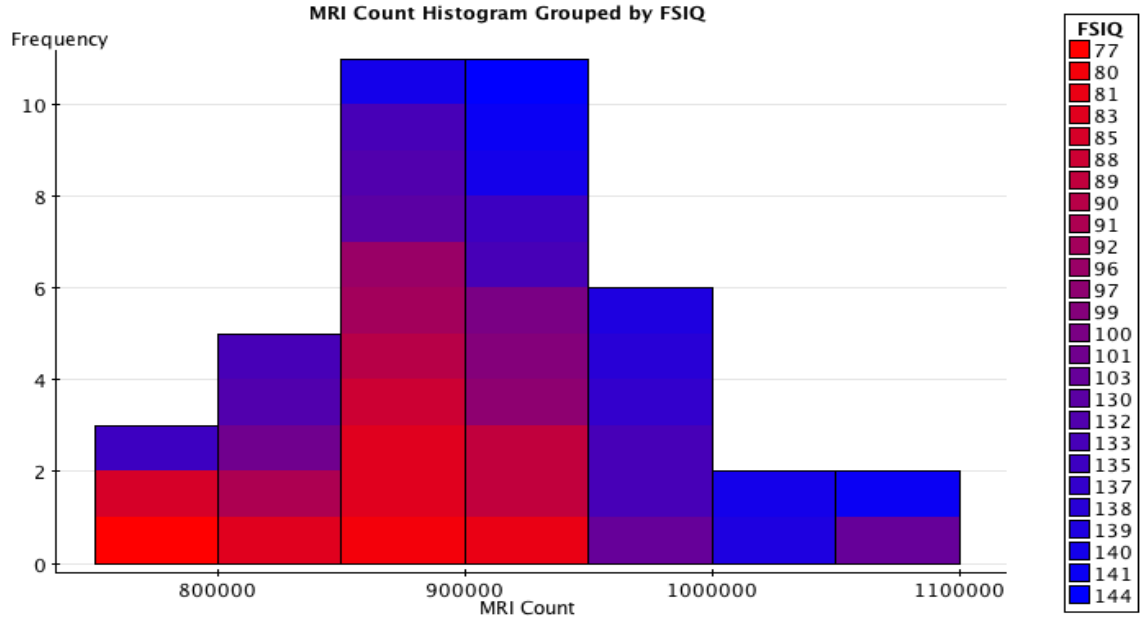

Fig. 6 MRI Count Histogram Grouped by FSIQ

The values of the MRI counts fit a normal curve as indicated by the histogram. When grouped by FSIQ scores, one can see that people with lower a MRI count generally has a lower FSIQ score. The same can be said of people with a higher MRI count and higher FSIQ score. Though there are several individuals that do not follow this trend precisely, this is to be expected because there are many other factors involved in intelligence other than brain size.

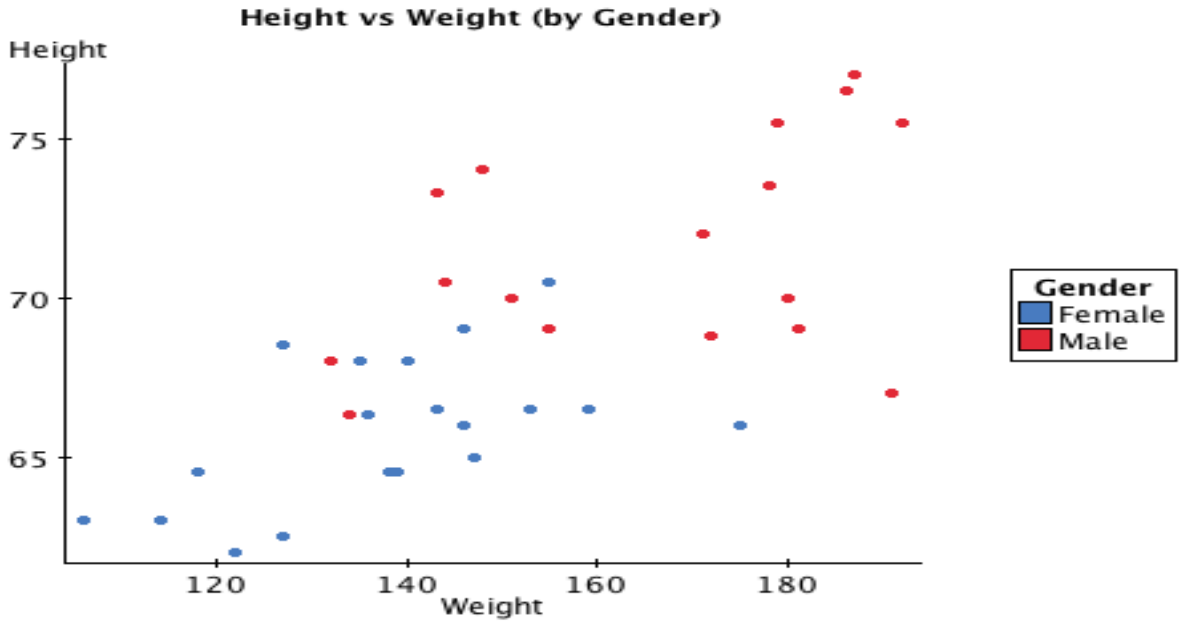

Fig. 7 Scatter Plot Height vs Weight

However, it is also curious to ask what differences there are between males and females. One could assume that because males are generally larger than females in body weight and height, that they will also have larger brain sizes.

ISSN 2348-1196 (print)
International Journal of Computer Science and Information Technology Research ISSN 2348-120X (online)
Vol. 2, Issue 3, pp: (328-338), Month: July - September 2014, Available at: www.researchpublish.com

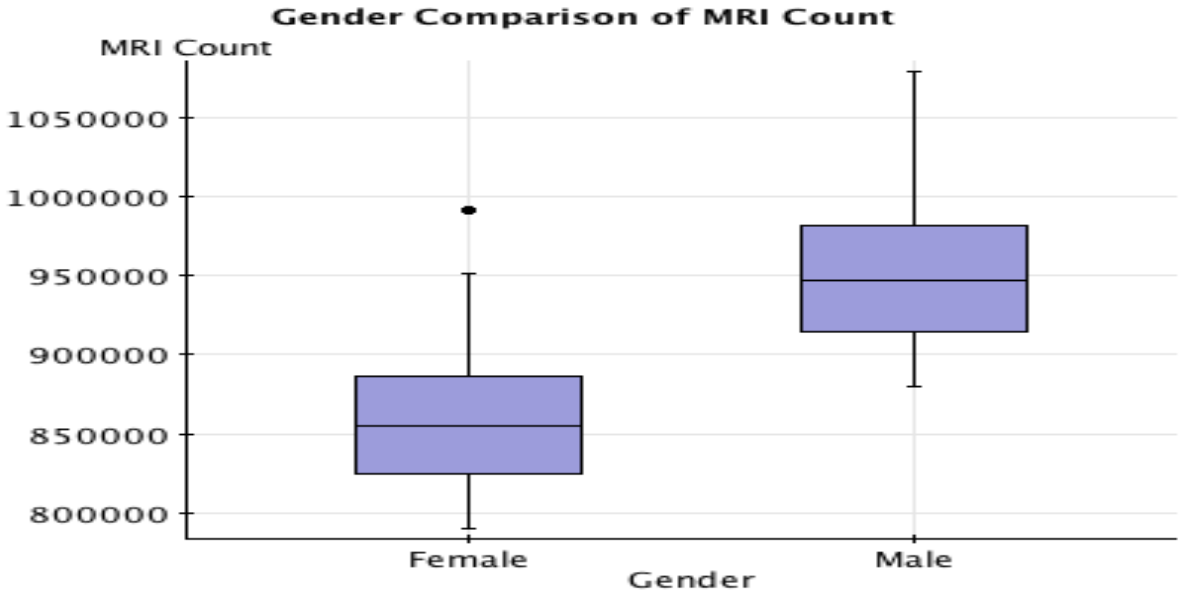

Fig. 8 Gender Comparison of MRI Count

Fig 8:In the above box plot, one can see that males tend to have larger brain sizes than females. Females have a median MRI count of 86,000 pixels, whereas males have a median of 94,000 pixels

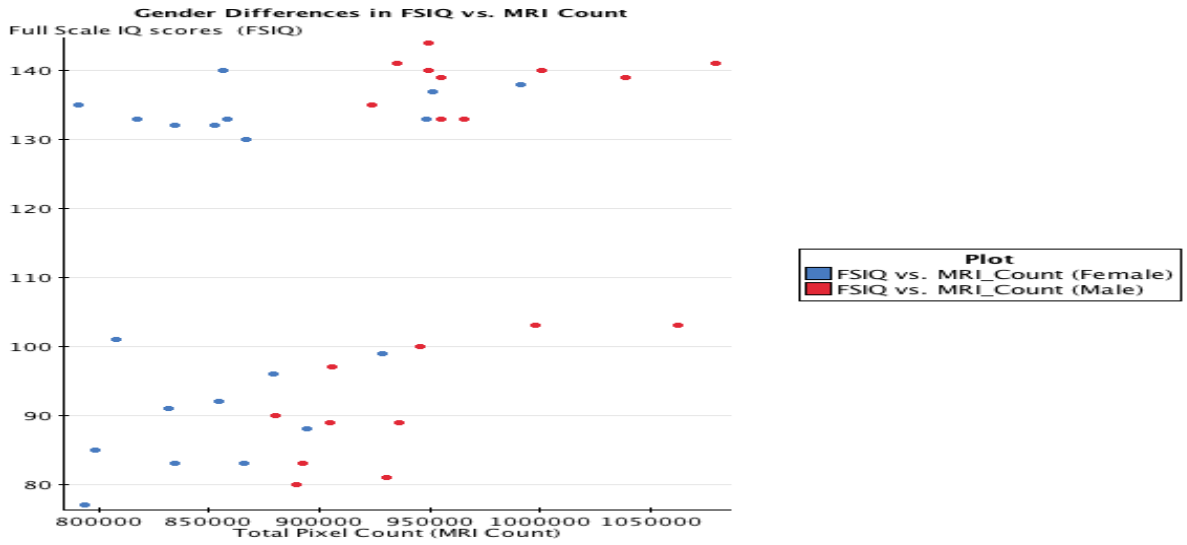

Fig. 9 Gender Differences in FSIQ vs. MRI Count

When plotting MRI count vs. FSIQ score, this scatter plot shows two main groups of data points, with a large gap between scores 104-130. Also, we see again that males generally have larger MRI counts than females, with a few exceptions. More importantly, however, the data show that as far as FSIQ scores are concerned, males and females are homogeneous.

VII. CONCLUSION

Observers in our study were successful in identifying faces based on our a priori thresholds. This was a surprising result to those of us who attempted the task and found it to be quite difficult. The fact that we used existing research MR data sets and the most basic, monochrome 3-D reconstructions may have biased our result. This bias, however, was in the direction of making the task more difficult and may explain our lower frequency of correct identification as compared with that reported by Chen et al. The results of both studies indicate that MR and CT facial reconstructions must be considered as equivalent to photographs for the purposes of human identification.

In this paper we have presented a review of current biometric identification technologies and suggested the potential of face and gait biometric traits for next generation biometric technologies. Some of work in progress in relation to development of face-gait fusion models, the importance of primary and secondary biometric traits and the role of fusion protocols in addressing the requirements of next generation biometrics is discussed. The future work will involve evaluation of fusion models being developed for different facegait databases in terms of false accept rates, false reject rates and equal error rates under controlled and uncontrolled environments.

REFERENCES

[1] Health Insurance Portability and Accountability Act of 1996, Pub. L. No. 104–191, 110 Stat. 1936, 1996.

[2] Standards for Privacy of Individually Identifiable Health Information; Final Rule. Title 45, Code of Federal Regulations, Parts 160 and 164, Aug. 2002.

[3] Bischoff-Grethe, I. B. Ozyurt, E. Bursa, B. T. Quinn, C. Fennema- Notestine, C. P. Clark, S. Morris, M.W. Bondi, T. L Jernigan, A. M. Dale, G. G. Brown, and B. Fischl, "A technique for the deidentification of structural brainMRimages," Hum. BrainMapping, vol. 28, no. 9, pp. 892– 903, Sep. 2007.

[4] J. Chen, K. Siddiqui, L. Fort, R. Moffitt, K. Juluru, W. Kim, N. Safdar, and E. Siegel, "Observer success rates for identification of 3D surfacereconstructed facial images and implications for patient privacy and security," in Proc. SPIE Int. Soc. Opt. Eng., 2007, pp. 65161B-1–65161B-8.

[5] R.A. Robb, D. P. Hanson, R. A. Karwoski, A. G. Larson, E. L.Workman, and M. C. Stacy, "ANALYZE:Acomprehensive, operator-interactive software package for multidimensional medical image display and analysis," Comput. Med. Imag. Graph., vol. 13, no. 6, pp. 433–445, 1989.

[6] V.Bruce, Z. Henderson, K. Greenwood, P. Hancock, M. Burton, and P. Miller, "Verification of face identities from images captured on video," J. Exp. Psychol.: Appl., vol. 5, no. 4, pp. 339–360, 1999.

[7] W. Zhao, R. Chellappa, A. Rosenfeld, and P. Phillips, "Face recognition: A literature survey," ACM Comput. Surv., vol. 35, pp. 399–458, 2003.

[8] C. Frowd, V. Bruce, A. McIntyre, and P. Hancock, "The relative importance of external and internal features of facial composites," Brit. J. Psychol., vol. 98, no. 1, pp. 61–77, Feb. 2007.

[9] J. Shepherd, G. Davies, and H. Ellis, "Studies of cue saliency," in Perceiving and Remembering Faces, G. Davies, E. Hadyn, and J. Shepherd, Eds. London: Academic, 1981, pp. 105–132.